EFFECT OF DEFORMATION ON SURFACE CHARACTERISTICS OF FINITE METALLIC CRYSTALS

V. V. POGOSOV, O. M. SHTEPA

Zaporizhzhya National Technical University,
(*64, Zhukovsky Str., Zaporizhzhya 69063, Ukraine; e-mail:vpogosov@zstu.edu.ua*)

UDC 537.533
‰ 2002

The surface stress and contact potential differences of elastically deformed faces of Al, Cu, Au, Ni, and Ti crystals are calculated within the modified stabilized jellium model using the self-consistent Kohn – Sham method. The obtained values of the surface stress are in agreement with the results of the available first-principle calculations. We find that the work function decreases/increases linearly with elongation/compression of crystals. Our results confirm that the available experimental data on contact potential difference obtained for a deformed surface by the Kelvin method correspond to a change of the surface potential rather than to a change of the work function. The problem of 'anisotropy" of the work function and ionization potential of a finite sample is discussed.

The preparation and study of nanometer scale structures attracts a considerable current interest for both technological and scientific reasons. The free-electron gas models are invariably popular tools in the physics of metals [1, 2] and low-dimensional structures [3].

Recently, several authors discussed the definition of the surface stress and the chemical potential in the case of finite samples [4–8]. In our previous papers [6, 8], we proposed a successful method to calculate the surface stress and the work function of a single elastically deformed finite metal crystal. It was applied for a simple metal. A fairly tightly bound '*d*" band that overlaps and hybridizes with a broader nearly free-electron '*sp*" band characterizes transition metals. The cohesive properties of simple, noble, and transition metals can be calculated from the first principles in the context of the one-electron picture provided by density-functional theory [9, 10].

The direct measurements, using the Kelvin method, showed a decreasing/increasing of the contact potential difference (CPD) of elastically tensed/compressed metal samples [11–14]. A similar effect on CPD was observed at the surface of samples with a nonuniform distribution of residual mechanical stresses [15]. The conventional method of measurement of the work function changes versus x-axis strain [11–14] is based on the expresion

$$\Delta W = - \mathrm{CPD}, \qquad (1)$$

i. e., the work function as if increases for a tensed sample. The change $\Delta W = W(u_{xx}) - W(0)$ was measured at the side perpendicular to the y- and z-directions, u_{xx} is the relative deformation along the x-axis (see Fig. 1). These, at first sight, surprising results mean that the work function increases/decreases with uniaxial tension/compression of a metallic sample. This fact contradicts another well-known observation: the work function of simple metals decreases for the transition $\mathrm{Al} \rightarrow \mathrm{Na} \rightarrow \mathrm{Cs}$, i. e., with decreasing the electron concentration.

In the present paper, we report the results of calculations of the effect of deformation on the surface energy, work function, and CPD of faces of technologically important metals such as Al, Ti, Ni, Cu, and Au using their nominal valence. The problem of accurate definition of the work function is discussed. We checked the accuracy of Eq. (1) by fully self-consistent calculations and showed that it is wrong. Eq. (1) is incorrect in the diagnostic of a strained surface.

1. Nonstrained Surface

Surface energy per unit area and work function are the most important characteristics of a metal surface. In the framework of density-functional theory, the total energy of metal is a functional of the nonhomogeneus electron concentration $n(r)$, $n(r) \rightarrow \bar{n}_0$ in bulk, $\bar{n}_0 = 3/(4\pi r_{s0}^3)$, $r_{s0} = Z^{1/3} r_0$, r_{s0} is the average distance between electrons in the nonstrained metal bulk, and Z is the metallic valence. Using the

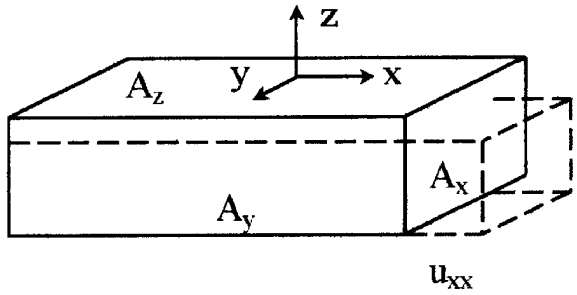

Fig. 1. Qualitative scheme of a sample tensed in the x-direction, $u_{xx} > 0$ is the relative deformation

pseudopotential approach, the total energy can be written as the sum

$$E[n(r)] = T_s + E_{\text{ex}} + E_{\text{cor}} + E_{\text{H}} + E_{\text{ps}} + E_{\text{M}}, \quad (2)$$

where T_s is the (non-interacting) electron kinetic energy, E_{ex} is the exchange energy, E_{cor} is the correlation energy, E_{H} is the Hartree (electrostatic) energy, E_{ps} is the pseudopotential correction, and E_{M} is the Madelung energy. The sum of first four terms in Eq. (2) corresponds to the energy of 'ordinary" jellium, E_J. The 'ordinary" jellium model provides a useful description for the bulk modulus and surface energy of simple metals only for $r_{s\,0} \approx 4$ bohr (Na), where the bulk jellium is stable. The jellium surface energy for $r_{s\,0} \leq 2$ and the bulk modulus for $r_{s\,o} \geq 5.5$ are negative. These deficiencies are removed in the stabilized jellium mode [17]. The average energy per valence electron in the bulk of stabilized jellium is $\bar{\varepsilon}_{SJ} = E[\bar{n}]/N$, where N is a total number of free electrons, defined by valence and atomic density,

$$\bar{\varepsilon}_{SJ} = \bar{\varepsilon}_J + \bar{w}_R + \bar{\varepsilon}_{\text{M}}, \quad (3)$$

where the term $\bar{\varepsilon}_J$,

$$\bar{\varepsilon}_J = \bar{t}_s + \bar{\varepsilon}_{\text{ex}} + \bar{\varepsilon}_{\text{cor}} = \frac{3}{10}\bar{k}_F^2 - \frac{3}{4\pi}\bar{k}_F + \bar{\varepsilon}_{\text{cor}}, \quad (4)$$

consists of the average kinetic, exchange, and correlation energy per electron, $\bar{k}_F = (3\pi^2 \bar{n}_0)^{1/3}$, r_0 is the radius of the Wigner – Seitz cell, and $\bar{w}_R = 2\pi\bar{n}_0 r_c^2$ represents the average of the repulsive part of the Ashcroft model potential, r_c is the radius of ionic core, $\bar{\varepsilon}_M = -9Z/10r_0$. We employ atomic units ($e = m = \hbar = 1$) throughout and the popular expression for the correlation energy [18, 19]

$$\bar{\varepsilon}_{\text{cor}} = -\frac{0.1423}{1 + 0.8293\bar{n}_0^{1/6} + 0.2068\bar{n}_0^{1/3}}. \quad (5)$$

Applying the variation principle, one can find the Euler – Lagrange equation for a nonhomogeneous electron gas

$$\mu = V_{\text{eff}}(r) + \frac{\delta T_s[n]}{\delta n(r)}, \quad (6)$$

where μ is the chemical potential of electrons, and effective one-electron potential is

$$V_{\text{eff}}(r) = \varphi(r) + \frac{\delta[E_{\text{ex}} + E_{\text{cor}}]}{\delta n(r)} + \langle \delta V \rangle_{\text{face}} \theta(r - r'), \quad (7)$$

where r' is the radius-vector of the surface, $\theta(r - r')$ is the step function. The electrostatic potential $\varphi(r)$ satisfies the Poisson equation

$$\nabla^2 \varphi(r) = -4\pi[n(r) - \rho(r)]. \quad (8)$$

The ionic charge distribution can be modeled by the step functional $\rho(r) = \bar{\rho}\theta(r - r')$, where $\bar{\rho} = \bar{n}_0/Z$, $\bar{n}_0$ is the electron concentration in the bulk.

The coordinate-independent term $\langle \delta V \rangle_{\text{face}}$ in Eq. (7) represents the difference between the pseudopotential of the ion lattice and the electrostatic potential of the positive background averaged over the Wigner – Seitz cell. This term allows one to distinguish different faces of semiinfinite samples. The face-dependence of the stabilization potential [16, 17] reads

$$\langle \delta V \rangle_{\text{face}} = \langle \delta V \rangle_{\text{WS}} - \left(\frac{\bar{\varepsilon}_{\text{M}}}{3} + \frac{\pi\bar{n}_0}{6} d_0^2 \right),$$

$$\langle \delta V \rangle_{\text{WS}} = \bar{n}_0 \frac{d}{d\bar{n}_0}(\bar{\varepsilon}_{\text{M}} + \bar{w}_R), \quad (9)$$

where d_0 is the spacing between the lattice planes parallel to the surface. From the bulk stability condition $d\bar{\varepsilon}_{SJ}/d\bar{n}_0 = 0$, one can obtained the relation

$$\langle \delta V \rangle_{\text{WS}} = -\bar{n}_0 \frac{d}{d\bar{n}_0}(\bar{t}_s + \bar{\varepsilon}_{\text{ex}} + \bar{\varepsilon}_{\text{cor}}). \quad (10)$$

The electronic profile $n(r)$ can be expressed in the terms of one-electron wave functions $\psi_i(r)$,

$$n(r) = \sum_{i=1}^{N} |\psi_i(r)|^2, \quad (11)$$

where the functions $\psi_i(r)$ satisfy the one-electron wave equation

$$\left[-\frac{1}{2}\nabla^2 + V_{\text{eff}}[r, n] \right] \psi_i(r) = \varepsilon_i \psi_i(r). \quad (12)$$

The set of the Kohn – Sham equations must be solved self-consistently. Then the total kinetic energy of electrons in Eq. (2) is

$$T_s[n] = \sum_{i=1}^{N} \varepsilon_i - \int n V_{\text{eff}}(r)\, d^3 r.$$

As a rule, it is supposed for semiinfinite metal that the electronic profile $n(r)$ and effective $V_{\text{eff}}(r)$ potential vary only in the direction perpendicular to the surface. The conventional approach involves introducing periodic boundary conditions in the x- and y-directions. Thus, the only crystal face is that in z-direction. In this case, the set of equations (8), (11), and (12) reduces to

$$\varphi(z) = \varphi(\infty) - 4\pi \int_{z}^{\infty} dz' \int_{z'}^{\infty} dz'' [n(z'') - \rho(z'')], \tag{13}$$

$$n(z) = \frac{1}{\pi^2} \int_{0}^{k_F} (\bar{k}_F^2 - k^2) [\psi_k(z)]^2 dk, \tag{14}$$

$$\left[-\frac{1}{2}\frac{d^2}{dz^2} + V_{\text{eff}}[z, n] \right] \psi_k(z) = \frac{1}{2} k^2 \psi_k(z). \tag{15}$$

Here, the effective potential is taken in the local-density-approximation

$$V_{\text{eff}}[z, n] = \varphi(z) + \frac{d[n(\varepsilon_{\text{ex}} + \varepsilon_{\text{cor}})]}{dn} + \\ + \langle \delta V \rangle_{\text{face}} \theta(-z), \tag{16}$$

where $n \equiv n(z)$. The electron wave number k varies in the interval $(0, \bar{k}_F)$. The solution of the problem can be reduced to the iteration procedure by means of the following relation [20]:

$$\varphi_{i+1}(z) = \int_{-\infty}^{\infty} dz' e^{-\bar{k}_F |z - z'|} \times \\ \times \left\{ \frac{2\pi}{\bar{k}_F} [n(z') - \rho(z')] + \frac{\bar{k}_F}{2} \varphi_i(z') \right\},$$

where i is the number of iterations.

The surface energy can be written as

$$\gamma_{SJ} = \gamma_J + \langle \delta V \rangle_{\text{WS}} \int_{-\infty}^{0} dz [n - \bar{n}_0]. \tag{17}$$

The ordinary jellium components are:

$$\gamma_s = \frac{1}{2\pi^2} \int_{0}^{k_F} \left[\frac{\pi}{4} - \delta(k) \right] k\, dk - \\ - \int_{-\infty}^{\infty} n [V_{\text{eff}}(z) - \bar{V}_{\text{eff}}]\, dz, \tag{18}$$

where δ is the phase shift of the wave function, $\psi_k(z) \to \sin[kz - \delta(k)]$, as $z \to -\infty$, $\bar{V}_{\text{eff}}$ is the bulk magnitude of the effective potential, $\bar{V}_{\text{eff}} \equiv V_{\text{eff}}(z = -\infty) < 0$, and

$$\gamma_{\text{ex, cor}} = \int_{-\infty}^{\infty} dz \{ n\varepsilon_{\text{ex, cor}} - \bar{n}_0 \bar{\varepsilon}_{\text{ex, cor}} \theta(-z) \}, \tag{19}$$

$$\gamma_{\text{H}} = \frac{1}{2} \int_{-\infty}^{\infty} dz \varphi [n - \rho]. \tag{20}$$

Putting the electrostatic potential in vacuum to be equal to zero, $\varphi(+\infty) = 0$, one can calculate the work function as ($\bar{\varepsilon}_F = \bar{k}_F^2 / 2$)

$$W_{z-\text{face}} \equiv -\mu = -\bar{V}_{\text{eff}} - \bar{\varepsilon}_F. \tag{21}$$

2. Deformed Surface

The strain dependence of the CPD was measured for polycrystalline compressed [11] and tensed samples [13, 14]. One can assume that a polycrystal is assembled from a number of simple crystallites. Thus, qualitatively, the problem can be reduced to the analysis of tension or compression applied to a single crystal. We consider a single crystal in the form of a parallelepiped with sides having equivalent Miller indices. For simplicity, the material of the sample is assumed to have the cubic crystallographic symmetry. We introduce the coordinate system with the axes x, y, and z perpendicular to the sample faces. Their areas are equal to A_x, A_y, and A_z, respectively (see Fig. 1). We neglect temperature and dimensional effects, which differs from the approach used in [3, 21].

Let us first express the average electron density in a metal as a function of deformation. For this purpose, consider an undeformed cubic cell of side length a_0, $a_0^3 = 4\pi r_0^3 / 3$. In the modified stabilized jellium model [6, 8], the metal energy is a function of the electron density parameter $r_{su} = Z^{1/3} r_{0u}$, spacing d_u between the lattice planes perpendicular to the z-direction, the Poisson ratio for a polycrystal ν, the Young's modulus Y, and deformation u_{xx}.

For a uniaxially deformed cell elongated or compressed along the x-axis, one can write [8]:

$$d_u = d_0 (1 - \nu u_{xx}), \tag{22}$$

where d_u is the spacing between the lattice planes perpendicular to the y- or z-directions, d_o is the interplanar spacing in an undeformed crystal,

$$\bar{n} = \bar{n}_0 [1 - (1 - 2\nu) u_{xx}] \tag{23}$$

is the average electron density in the deformed metal bulk, ν is the Poisson ratio for a polycrystal, and the corresponding density parameter is

$$r_{su} = r_s\left(1 + \frac{1-2\nu}{3}u_{xx}\right). \quad (24)$$

The stabilization potential (10) must be changed by

$$\langle \delta V \rangle_{WS} = -\bar{n}_0 \frac{d}{d\bar{n}_o}\left(\bar{t}_s + \bar{\varepsilon}_{ex} + \bar{\varepsilon}_{cor} + \frac{P}{\bar{n}}\right), \quad (25)$$

where $P = -Yu_{xx}(1-2\nu)$ is the external pressure.

An applied force stimulates a change of the volume and reticular electron density at the particular faces of a neutral metallic crystal and results in a difference between electrostatic potentials of these faces. The corresponding anisotropic three-dimensional electric field arises due to a transfer of electrons between the faces. Thus, finite sample sizes lead, in the first place, to the fact that the surface tends to equipotentiality. In general case, this transfer of electrons does not give any possibility to calculate the work function using the conventional approach for a semiinfinite sample. However, in the special case of the largest face of the metallic crystal,

$$A_z >> A_x, A_y, \quad (26)$$

the use of the conventional approach (see Eq. (21)) is adequate in fact. As a result, the calculated work function exclusively for the *z*-direction corresponds to that for the *whole* crystal. The face perpendicular to this direction is not appreciably perturbed by the transferred electronic charge indepedently of the crystallographic orientation [8]. The conventional method involves introducing periodic boundary conditions in the *x*- and *y*-directions. In this case, the surface potential depends strongly on the atomic packing density. Thus, the only crystal face is that in the *z*-direction. Putting the three-dimensional electrostatic potential in vacuum to be equal to zero, one can use definition (21) under condition (26), where the effective potential in the bulk of a semiinfinite metal $\bar{V}_{eff}$ yields the *total* sample-vacuum barrier. Solving the set of equations (13)–(16) and using relations (22)–(25), one can calculate the strain dependences of the surface energy and work function.

We calculate the diagonal *xx*-component of the surface stress for the given largest face using the following expression [5–8]:

$$\tau_{xx} = \gamma + \frac{d\gamma}{du_{xx}}, \quad (27)$$

where γ is the surface energy per unit area of the largest face of the sample.

3. Results and Discussions

We performed our calculations for the work function and surface energy in the case of absence of the strain state of metals and for the strain dependences $W_{face}(u_{xx})$ and $\gamma_{face}(u_{xx})$ within the range of deformation $-0.01 \le u_{xx} \le +0.01$ for Ni and

Calculated surface energy γ and work function $W(u_{xx}=0)$. The experimental values of *B*, γ, *W* for polycrystaline metal, the Poisson ratio ν, and the Young's modulus *Y* necessary in the calculation of the strain dependences are taken from [23–25]

Metal	r_0 (bohr)	*Z*	*B* (MBar)		Face	γ (erg/cm^2)		*W* (eV)		ν	*Y* (GPa)
			theory	exp.		theory	exp.	theory	exp.		
Al	2.985	3	1.565	0.722	*fcc* (100) *fcc* (110) *fcc* (111)	1087 1683 939	1160	3.806 3.643 4.119	4.25	0.34	62.5 71.4 75.1
Au	3.010	3 (1)	1.519 (0.202)	1.732	*fcc* (100) *fcc* (110) *fcc* (111)	1069 (395) 1652 (440) 924 (383)	1134	3.792 (3.318) 3.630 (3.148) 4.105 (3.478)	4.30	0.42	43.5 81.3 115.0
Ni	2.610	3	2.567	1.860	*fcc* (100) *fcc* (110) *fcc* (111)	1376 2224 1162	1810	4.010 3.858 4.325	4.50	0.32	138.0 215.0 262.0
Cu	2.660	2	1.113	1.370	*fcc* (100) *fcc* (110) *fcc* (111)	979 1295 899	1351	3.855 3.647 4.123	4.40	0.35	65.8 131.0 194.0
Ti	3.040	4	2.545	1.051	*hcp* (0001) *fcc* (100) *fcc* (110) *fcc* (111)	1081 1355 2456 1081	2200	4.205 3.865 3.774 4.205	3.95	0.30	145.0 96.1 96.1 27.8

$-0.03 \le u_{xx} \le +0.03$ for Al, Au, Cu, and Ti, respectively. The positive/negative deformation u_{xx} is equivalent to the tension/compression of the largest side of the sample, i. e., the decrease/increase of the atomic packing density at this side, and the decrease/increase of the mean electron concentration and the interplanar spacing in the z-direction. The upper side of the sample in Fig. 1 is suggested to have indices (100) or (110), (111), (0001).

The tendencies in the bulk surface characteristics of Al, Au, Cu, Ni, and Ti have been reproduced from the theory of uniform electron gas with the average electron density corresponding to the nominal valence by the volume per atom. The use of the integer and fractional magnitude of a valency leads to a successful calculation of the bulk modulus B [22]. The concept of metallic valency can be defined to treat simple and transition metals in terms of the uniform electron gas.

The results of our calculations for free and deformed faces are summarized in Table and Figs. 2 and 3, respectively. For comparison, we perform the calculations of the bulk modulus $B = \bar{n}_0^{2} d^2(\bar{n}_0^{2}\bar{\varepsilon}_{SJ})/d\bar{n}_0^{2}$, γ and W for Au ($Z = 1$). The data of Table demonstrate the intricate picture for a common description of cohesive and surface metallic properties in the simple approach. In fact, the use of nominal valence gives satisfactory results for the surface characteristics. We found that the deformation changes of the work function and the surface energy remain linear with respect to the deformation. The strain derivative of the work function and the surface energy is positive. The values of the surface stress component τ_{xx} vary appreciably within the interval $(1.15,\ 1.75)\gamma_{\text{face}}$. Similar results for the surface stress (1250 and 1440 erg/cm^2 for Al (111)) are yielded by the *ab initio* [26] and atomistic [27] calculations. In contrast to the present work (Fig. 2), the strain derivative $d\gamma/du_{xx}$ obtained for Au in [28] was larger than the surface energy γ.

The relative change of the work function equals approximately 1% for the maximal strains (compare Table and Fig. 3). In the case of compression ($u_{xx} < 0$), the tails of the electron profile and, therefore, effective potential grow steeper in vacuum. In the case of tensile strain ($u_{xx} > 0$), these coordinate dependences have the opposite tendency. A total decrease/increase of the work function W is determined by a positive/negative shift of the effective potential versus strain in the bulk of metal (neglecting the deformation dependence $\varepsilon_F(u_{xx})$, one can certainly put the shift $\Delta W \approx -\Delta\bar{V}_{\text{eff}}$). Our calculation mimics the usual work function dependence on electronic concentration (for the 'transition" $\text{Al} \to \text{Na} \to \text{Cs}$). However, relation (1) gives the incorrect dependence $W(u_{xx})$. These results contradict, at first look, experiments [11–14].

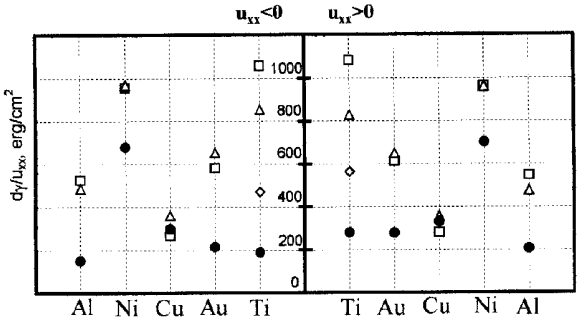

Fig. 2. Calculated derivative $d\gamma/du_{xx}$ for estimation of the surface stress, Eq. (26). The left and right parts of the figure correspond to the compression ($u_{xx} < 0$) and the tension ($u_{xx} > 0$) of the sample, respectively

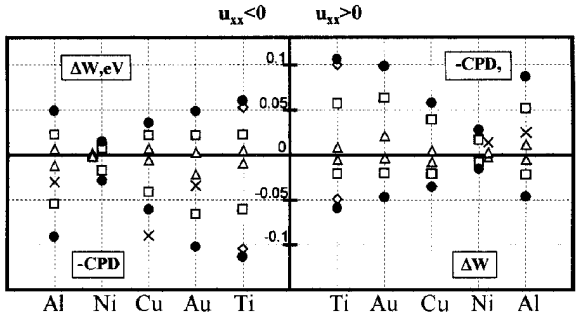

Fig. 3. Calculated change of the work function and the contact potential difference for the maximal strain of elastically deformed largest faces (Fig. 1). The experimental values of CPD are taken from [11] for compressed ($u_{xx} = -0.03$) polycrystalline Al, Cu, and Au samples and from [13, 14] for tensed Al ($u_{xx} = +0.03$) and Ni ($u_{xx} = +0.01$) samples (see also Table in [29]). The values of CPD for negative deformation are extracted from the lowest experimental shifts in contact potential (measured in units of $\mu\text{Vcm}^2/\text{kg}$) of [11] multiplied by $Y_{\text{av}}|u_{xx}|$, where $Y_{\text{av}} = 1/3\,(Y_{100} + Y_{110} + Y_{111})$. Note that the values of CPD and ΔW were erroneously equated in [11–15]

We suggest that, qualitatively, the problem is reduced to the effect of strain on a single crystal. The experimental observations can be explained by basing on the change of the effective potential at the position of the image plane $z = z_0$ [8]. For simplicity, we take $z_0 = 1$bohr for faces and use $\text{CPD} = \Delta V_{\text{eff}}(u_{xx}, z_0)$. At present, we calculated ΔW and CPD without use of Eq. (1). Our Fig. 3 demonstrates, on the one hand, a good qualitative agreement of the calculated values of $\text{CPD}(u_{xx})$ with the experimental data and, on the other hand, the *inverse* dependence $W(u_{xx})$ than that following from Eq. (1). The analysis of experimental data provided the evidence for that it is not adequate to use the Kelvin method for the measurement, e. g.,

of the temperature dependence of the work function (see [30, Fig. 6]).

Our results show: (i) the strain changes of the effective potential in the bulk and at the surface have the opposite sings, (ii) the sign of the deformation effect is independent of the material and crystallographic orientation.

In conclusion, let us recall that the density-functional calculations of this quantity deal with nonrealistic semiinfinite systems. However, in all experiments, *finite* samples are used, in general, of arbitrary sizes and shapes. In this context, an important remark appears about the conventional definition of face-dependent work function. The ionization potential (IP) of a finite sample (as a 'giant molecule“) is given by

$$\mathrm{IP} = E_{N-1} - E_N \approx W + \frac{e^2}{2C}, \qquad (28)$$

where E_N is the total energy of a neutral metallic sample containing N electrons. Here W is introduced as the work function of the *whole* sample and C is a capacitance of the sample, which is a scalar quantity. It is clearly seen from Eq. (28) that the work function is not an 'anisotropic“ characteristic but a scalar quantity, and $\mathrm{IP} \to W$ at $C \to \infty$. It may be demonstrated by formation of a finite sample adding consistently atoms each to other. The ionization potential of a single atom, dimer, etc. (up to work function) corresponds to the ionization process of each stage of nucleation (up to the solid) [31]. Thus, the conventional definition (28) leads to the conclusion that the concept of an anisotropy of the work function of metal is spurious in principle. Hence, the realistic geometric considerations presented in the [16, 32] are adequate in the case when all sample faces are possess the same atomic packing density.

This work was supported by the Ministry of Education and Science of Ukraine and the NATO 'Science for Peace“ Programme. We thank V.U. Nazarov for giving us an access to his computer code for testing purposes and W.V. Pogosov for reading the manuscript.

1. *Sahni V., Solomatin A.* // Adv. Quant. Chem. – 1999. – **33**. – P.241–271.
2. *Shore H.B., Rose J.H.* // Phys. Rev. B. – 1999. – **59**, N16. – P.10458–10492.
3. *Pogosov V.V., Kotlyarov D.P., Kiejna A., Wojciechowski K.F.* // Surf. Sci. – 2001. – **472**. – P.172–176.
4. *Pogosov V.V., Pogosov W.V., Kotlyarov D.P.* // Zh. Eksp. Teor. Fiz. – 2000. – 117, N 5. – P.1043–1053.
5. *Sanfeld A., Steinchen A.* // Surf. Sci. – 2000. – **463**. – P.157–173.
6. *Kiejna A., Pogosov V.V.* // Phys. Rev. B. – 2000. – **62**, N15. – P.10445–10450.
7. *Bottlomey D.J., Ogino T.* // Ibid. – 2001. – **63**. – P.165412.
8. *Pogosov V.V., Kurbatsky V.P.* // Zh. Eksp. Fiz. – 2001. – **119**, N2. – P.350–358.
9. *Moruzzi V.L., Jenak J.F., Williams A.R.* Calculated Electronic Properties of Metals. – New York: Pergamon, 1978.
10. *Wills J.M., Harrison W.A.* // Phys. Rev. B. – 1983. – **28**. – P.4363–4368.
11. *Craig P.P.* // Phys. Rev. Lett. – 1969. – **22**. – P.700–703.
12. *Mints P.I., Melekhin V.P., Partensky M.B.* // Fizika Tverd. Tela. – 1974. – **16**, N12. – P.3584–3586.
13. *Pogosov V.V., Levitin V.V., Loskutov S.V.* // JTP Lett. – 1990. – **16**, N3. – P.14–17.
14. *Loskutov S.V.* // Fiz. Met. i Metalloved. – 1998. – **86**, N2. – P.149–152.
15. *Levitin V.V., Loskutov S.V., Pravda M.I., Serpetsky B.A.* // Nondestr. Test. Eval. – 2001. – **17**. – P.79–89.
16. *Lang N.D., Kohn W.* // Phys. Rev. B. – 1971. – **3**, N4. – P.1215–1223.
17. *Perdew J.P.* // Prog. Surf. Sci. – 1995. – **48**, N1–4. – P.245–259.
18. *Ceperley D.M., Alder B.J.* // Phys. Rev. Lett. – 1980. – **45**. – P.510–515.
19. *Perdew J.P., Zunger A.* // Phys. Rev. B. – 1981. – **23**. – P.5048–5055.
20. *Manninen M., Nieminen R., Hautojarvi P., Arponen J.* // Ibid. – 1975. – **12**, N10. – P.4012–4022.
21. *Pogosov V.V., Kotlyarov D.P., Mileshkina N.V. et al.* // Phys. Low-Dimen. Struct. – 2000. – **7/8**. – P.91–104.
22. *Wojciechowski K.* // Physica. B. – 1996. – **229**. – P.55–62.
23. *Fomenko V.S.* Emission Properties of Metals. – Kiev: Naukova Dumka, 1980.
24. *Tables* of Phyisical Values / Ed. by I.K. Kikoin. – Moskow: Atomizdat, 1976.
25. *Cohesion* in Metals / F.R. de Boer, R. Boom, W.C.M. Mattens et al. – Amsterdam: North-Holland, 1988.
26. *Needs R.J., Godfrey M.J.* // Phys. Rev. B. – 1990. – **42**. – P. 10933–10940.
27. *Feibelman P.J.* // Ibid. – 1994. – **50**. – P.1908–1913.
28. *Needs R.J., Mansfield M.* // J. Phys.: Condens. Matter. – 1989. – **1**. – P.7555–7566.
29. *Pogosov V.V.* // Solid State Communs. – 1992. – **81**. – P.129–133.
30. *Durakiewicz T., Arko A.J., Joyce J.J. et al.* // Surf. Sci. – 2001. – **478**. – P.72–82.
31. *Frenkel Ya.I.* Introduction in the Theory of Metals. – Moscow: GIFML, 1958. – Ch. 2.
32. *Smoluchowski R.* // Phys. Rev. – 1941. – **60**, N1. – P.661–674.

Received 22.03.02